AIMS Mathematics, 8(12): 31258–31267.
DOI:10.3934/math.20231600
Received: 06 June 2023
Revised: 08 November 2023
Accepted: 15 November 2023
Published: 24 November 2023

http://www.aimspress.com/journal/Math

Research article

Inversion formulas for quarter-spherical Radon transforms

Gyeongha Hwang[1] **and Sunghwan Moon**[2,*]

[1] Department of Mathematics, Yeungnam University, Gyeongsan 38541, Republic of Korea
[2] Department of Mathematics, Kyungpook National University, Daegu 41566, Republic of Korea

* **Correspondence:** Email: sunghwan.moon@knu.ac.kr.

Abstract: The applications of spherical Radon transforms include synthetic aperture radar, sonar tomography, and medical imaging modalities. A spherical Radon transform maps a function to its integrals over a family of spheres. Recently, several types of incomplete spherical Radon transforms have received attention in research. This study examines two types of quarter-spherical Radon transforms that assign a function to its integral over a quarter of a sphere: 1) center of a quarter sphere of integration on a plane, and 2) center on a line and the rotation of the quarter sphere. Furthermore, we present inversion formulas for these two quarter-spherical Radon transforms.

Keywords: photoacoutic; tomography; Radon transform; inversion; a quarter sphere
Mathematics Subject Classification: 35L05, 44A12

1. Introduction

A spherical Radon transform maps a function to its integral over a family of spheres. The problem of inverting a spherical Radon transform from a set of integrals along all spheres is overdetermined as the family of all spheres in $\mathbb{R}^n, n \geq 2$, is determined using $(n+1)$-dimensional variables. Hence, spherical Radon transforms can be inverted in numerous ways from a set of integrals along some spheres. The centers of the spheres are centered at any point in the whole space with a fixed radius [39], or all spheres of integration pass through the origin [3, 4, 25, 30, 31]. In case of a variable radius, the centers can also be restricted on a hyperplane [2, 7, 27, 32, 38], a sphere [8, 9, 26, 40], a cylinder [13, 20], etc. [12, 18, 19, 28, 36].

The relevance of the spherical Radon transform to solving the wave equation has garnered significant interest in the context of Partial Differential Equations (PDEs) [5]. This interest has grown as the wave equation became intertwined with fields such as sonar, seismic waves and radar [7, 29]. For example, a simplified model of Photoacoustic Tomography can be described as follows [1, 17, 24]: When a body of interest is irradiated with short pulses of electromagnetic waves, some of the radiation

is absorbed by the body and heats the tissue. As a result, the body experiences thermoelastic expansion and ultrasound waves are produced. Transducers placed at the boundary of the body record this ultrasound. Assuming that the speed of the ultrasound is a constant c, at any instant t, one transducer records several signals generated by a location at a fixed distance ct from the detector. In other words, the detector measurements can be represented as the integral of a function along a sphere centered at the detector location with varying radii (depending on time). We can measure enough data using an array of these transducers (or by moving the detector to the boundary surface) to recover an unexposed image function that essentially contains the biological information of the body. As similar mathematical problems arise in other imaging models, such as sonar and radar imaging, the inversion of spherical Radon transforms has become a subject of considerable interest.

Recent research has also explored incomplete spherical Radon transforms. For instance, restrictions have been imposed on the set of radii of integration spheres [1,11]. Another variant is the spherical-cap Radon transform, which assigns a given function f to its integrals over a part of a sphere of integration, rather than the entire sphere [11,33], (where limited angular-aperture detectors are employed, similar to [15,35]). While the uniqueness of the spherical-cap Radon transform has been established, obtaining an exact inversion formula remains a challenge to the best of our knowledge.

In this study, we investigate two types of quarter-spherical Radon transforms whose integrals are a quarter of a sphere: 1) centers of spheres of integration lie on a plane, and 2) centers of spheres of integration lie on a line and a quarter sphere of integration revolves around the line. To our knowledge, we are the first to study these types of Radon transforms and find the exact inversion formulas. These quarter-spherical Radon transforms are developed from endoscopic photoacoustic imaging that can provide structural and functional information of biological luminal structures such as the coronary arteries and digestive tract [14, 16, 22, 34, 37, 41]. In [34], the author built a forward imaging model and inverted the forward model through iterative optimization, and in [41], a Convolutional Neural Network (CNN) based on deep gradient descent was developed. Assuming our model is successful, our results help reconstruct higher quality images than [34] and provide a theory as to why CNNs [41] work.

The shape of the detector is frequently depicted in endoscopic photoacoustic images as a pentahedron with two right-triangle faces, as shown in Figure 1(a); for the design of an actual detector, see [37] Figure 1. The motion of the detector corresponds to one of the centers of the integral sphere, and the time may vary with radius. We study the quarter-spherical Radon transforms for reasons that may be somewhat related to endoscopic photoacoustic imaging. However, it is reasonable that these transforms could appear in photoacoustic imaging using pentahedron detectors, like a spherical-cap Radon transform arises in one with a specific detector [33]. Additionally, such a problem of determining a function from the integral value on a particular family of manifolds is known as the integral geometry problem [10, 21]; it is a complex task that is worth studying.

The rest of this paper is organized as follows. Quarter-spherical Radon transforms are precisely formulated in Section 2. Two inversion formulas for the two types of quarter-spherical Radon transforms are derived in Section 3. The paper concludes with a short discussion in Section 4.

2. Formulation of the quarter-spherical Radon transform

In this section, we define two quarter-spherical Radon transforms. First, let us define a quarter-spherical Radon transform with the centers of integration spheres on the hyperplane for the n dimensions, as follows:

Definition 1. *For* $(\mathbf{u}, r) \in \mathbb{R}^{n-1} \times [0, \infty)$*, the quarter-spherical Radon transform of* f *on the hyperplane is defined as*

$$R_H f(\mathbf{u}, r) = r^{1-n} \int_{S^{n-1}_{r,q}} f(\mathbf{u} + \mathbf{x}, z) \mathrm{d}S(\mathbf{x}, z), \quad (\mathbf{u}, r) \in \mathbb{R}^{n-1} \times [0, \infty),$$

where $\mathrm{d}S(\mathbf{x}, z)$ is the surface measure on the sphere and $S^{n-1}_{r,q} = \{(\mathbf{x}, z) \in \mathbb{R}^n : |(\mathbf{x}, z)| = r, x_1 > 0, z > 0\}$ if the integral exists (see Figure 1(b) for $n = 3$).

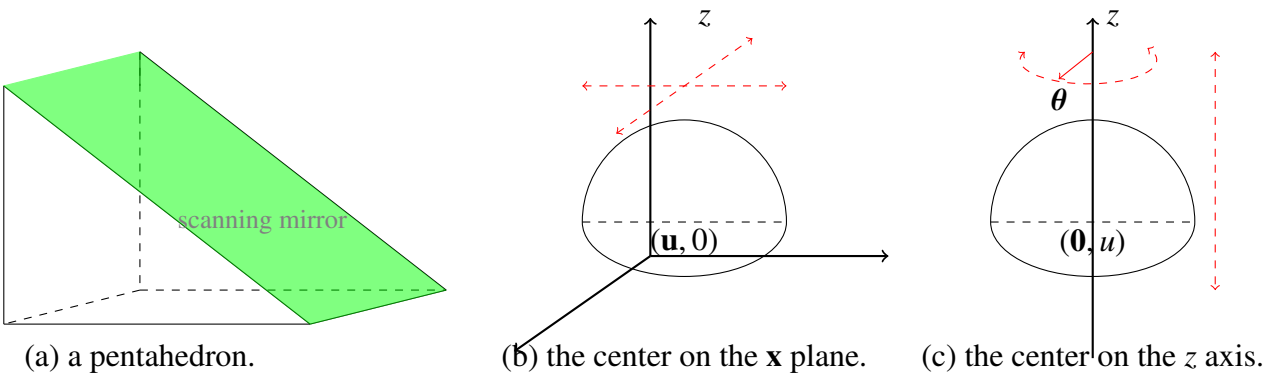

(a) a pentahedron. (b) the center on the $\mathbf{x}$ plane. (c) the center on the z axis.

Figure 1. A pentahedron and quarter sphere of integration.

Next, let us define the quarter-spherical Radon transform with the centers of integration spheres on a line and the rotation of a quarter sphere, as follows:

Definition 2. *For* $(u, \theta, r) \in \mathbb{R}^1 \times [0, 2\pi) \times [0, \infty)$*, the quarter-spherical Radon transform of* f *is defined as*

$$R_L f(u, \theta, r) = \frac{1}{r^2} \int_{S^2_{\theta,r,q}} f(\mathbf{x}, z + u) \mathrm{d}S(\mathbf{x}, z),$$

where $S^2_{\theta,r,q} = \{(\mathbf{x}, z) \in \mathbb{R}^3 : |(\mathbf{x}, z)| = r, z > 0, (\cos\theta, \sin\theta) \cdot \mathbf{x} > 0\}$ if the integral exists (see Figure 1(c)).

Actually, we are interested in the 3 dimension cases for $R_H f$ and $R_L f$, but the inversion of $R_H f$ can be easily generalized, and the inversion of $R_L f$ requires an inversion formula for 2 dimension $R_H f$. Therefore, for $R_L f$, only the 3 dimension case is discussed.

3. Inversion formulas

In this section, we derive inversion formulas for two quarter-spherical Radon transforms. We first develop an inversion formula for the quarter-spherical Radon transform $R_H f$. For finding the inversion

formula for $R_L f$, we need an inversion formula for the quarter-spherical Radon transform $R_H f$ when considering $n = 2$.

Theorem 3. *For $f \in C(\mathbb{R}^n)$ with compact support in $\{(\mathbf{x}, z) \in \mathbb{R}^n : z \geq 0\}$, we have*

$$f(\mathbf{x}, z) = \frac{4z}{(2\pi)^n} \int_{\mathbb{R}} \int_{\mathbb{R}^{n-1}} e^{\mathrm{i}\left(\mathbf{x}\cdot\boldsymbol{\xi} + z^2\sigma - \frac{|\boldsymbol{\xi}|^2}{4\sigma}\right)} \left(\frac{\mathrm{i}\sigma}{\pi}\right)^{\frac{n-1}{2}} \left(1 + \operatorname{erf}\left(-\frac{\xi_1\sqrt{\mathrm{i}}}{2\sqrt{\sigma}}\right)\right)^{-1} \times \int_0^\infty \mathcal{F}_{n-1}(R_H f)(\boldsymbol{\xi}, r) e^{-\mathrm{i}r^2\sigma} r^{n-1} \mathrm{d}r\mathrm{d}\boldsymbol{\xi}\mathrm{d}\sigma, \tag{3.1}$$

where $\mathcal{F}_{n-1}$ is the $n-1$-dimensional Fourier transform and erf is the error function defined as $\operatorname{erf} z = \frac{2}{\sqrt{\pi}} \int_0^z e^{-t^2} \mathrm{d}t^*$.

Proof. By definition, $R_H f$ can be written as

$$r^{2-n} \int_{|\mathbf{x}| \leq r, x_1 > 0} f(\mathbf{x} + \mathbf{u}, \sqrt{r^2 - |\mathbf{x}|^2}) \frac{\mathrm{d}\mathbf{x}}{\sqrt{r^2 - |\mathbf{x}|^2}}. \tag{3.2}$$

Let us define the function F on $\mathbb{R}^n$ by

$$F(\mathbf{x}, z) = \begin{cases} \dfrac{f(\mathbf{x}, \sqrt{z})}{\sqrt{z}} & \text{if} \quad z > 0, \\ 0 & \text{otherwise.} \end{cases}$$

Then, we have $f(\mathbf{x}, z) = zF(\mathbf{x}, |z|^2)$ for $z \geq 0$. Substituting F into (3.2) gives

$$R_H f(\mathbf{u}, r) = r^{2-n} \int_{|\mathbf{x}| \leq r, x_1 > 0} F(\mathbf{x} + \mathbf{u}, r^2 - |\mathbf{x}|^2) \mathrm{d}\mathbf{x}.$$

Taking the $n-1$-dimensional Fourier transform of $R_H f$ with respect to $\mathbf{u}$, we have

$$r^{n-2} \mathcal{F}_{n-1}(R_H f)(\boldsymbol{\xi}, r) = \int_{|\mathbf{x}| \leq r, x_1 > 0} \mathcal{F}_{n-1} F(\boldsymbol{\xi}, r^2 - |\mathbf{x}|^2) e^{\mathrm{i}\boldsymbol{\xi}\cdot\mathbf{x}} \mathrm{d}\mathbf{x},$$

where $\mathcal{F}_{n-1}(R_H f)$ and $\mathcal{F}_{n-1} F$ are the $n-1$-dimensional Fourier transforms of $R_H f$ and F with respect to $\mathbf{u}$ and $\mathbf{x}$, respectively.

By multiplying $re^{r^2(-\mathrm{i}\sigma - \epsilon)}$ for $\epsilon > 0$ and integrating with respect to r, we have

$$\begin{aligned} \int_0^\infty \mathcal{F}_{n-1}(R_H f)(\boldsymbol{\xi}, r) e^{r^2(-\mathrm{i}\sigma-\epsilon)} r^{n-1} \mathrm{d}r &= \int_0^\infty \int_{|\mathbf{x}| \leq r, x_1 > 0} \mathcal{F}_{n-1} F(\boldsymbol{\xi}, r^2 - |\mathbf{x}|^2) e^{\mathrm{i}\boldsymbol{\xi}\cdot\mathbf{x}} e^{r^2(-\mathrm{i}\sigma-\epsilon)} r \mathrm{d}\mathbf{x}\mathrm{d}r \\ &= \int_{\mathbb{R}_+^{n-1}} \int_{|\mathbf{x}|}^\infty \mathcal{F}_{n-1} F(\boldsymbol{\xi}, r^2 - |\mathbf{x}|^2) e^{\mathrm{i}\boldsymbol{\xi}\cdot\mathbf{x}} e^{r^2(-\mathrm{i}\sigma-\epsilon)} r \mathrm{d}r\mathrm{d}\mathbf{x}, \end{aligned} \tag{3.3}$$

*for details of the error function see [23, Chapter 2]

where $\mathbb{R}^{n-1}_+ = \{\mathbf{x} \in \mathbb{R}^{n-1} : x_1 > 0\}$. Changing the variables $r^2 - |\mathbf{x}|^2 \to t$ gives

$$\begin{aligned}\int_0^\infty \mathcal{F}_{n-1}(R_H f)(\boldsymbol{\xi}, r) e^{r^2(-\mathrm{i}\sigma-\epsilon)} r^{n-1} \mathrm{d}r &= 2^{-1} \int_{\mathbb{R}^{n-1}_+} \int_0^\infty \mathcal{F}_{n-1} F(\boldsymbol{\xi}, t) e^{\mathrm{i}\boldsymbol{\xi}\cdot\mathbf{x}} e^{-\mathrm{i}(t+|\mathbf{x}|^2)(\sigma-\mathrm{i}\epsilon)} \mathrm{d}t\mathrm{d}\mathbf{x} \\ &= 2^{-1} \int_{\mathbb{R}^{n-1}_+} \int_{\mathbb{R}} \mathcal{F}_{n-1} F(\boldsymbol{\xi}, t) e^{\mathrm{i}\boldsymbol{\xi}\cdot\mathbf{x}} e^{-\mathrm{i}(t+|\mathbf{x}|^2)(\sigma-\mathrm{i}\epsilon)} \mathrm{d}t\mathrm{d}\mathbf{x}.\end{aligned}$$

The last equality follows from the compact support of F on $z > 0$. Hence, it holds that

$$\int_0^\infty \mathcal{F}_{n-1}(R_H f)(\boldsymbol{\xi}, r) e^{r^2(-\mathrm{i}\sigma-\epsilon)} r^{n-1} \mathrm{d}r = 2^{-1} \int_{\mathbb{R}^{n-1}_+} e^{\mathrm{i}\boldsymbol{\xi}\cdot\mathbf{x}} e^{-|\mathbf{x}|^2(\mathrm{i}\sigma+\epsilon)} \mathrm{d}\mathbf{x}\, \mathcal{F}_n F(\boldsymbol{\xi}, \sigma - \mathrm{i}\epsilon), \tag{3.4}$$

where $\mathcal{F}_n F$ is the n-dimensional Fourier transform of F. To compute the integral with respect to $\mathbf{x}$, we employ the following identities [6, (11) on page 15 and (18) on page 73]: for $\operatorname{Re} a > 0$,

$$\int_0^\infty e^{-x^2 a} \cos(x\xi) \mathrm{d}x = \frac{1}{2}\left(\frac{\pi}{a}\right)^{\frac{1}{2}} e^{-\frac{\xi^2}{4a}} \text{ and } \int_0^\infty e^{-x^2 a} \sin(x\xi) \mathrm{d}x = -\frac{\mathrm{i}}{2}\left(\frac{\pi}{a}\right)^{\frac{1}{2}} e^{-\frac{\xi^2}{4a}} \operatorname{erf}\left(\frac{\mathrm{i}a^{-\frac{1}{2}}\xi}{2}\right), \tag{3.5}$$

where $\operatorname{Re} a$ is the real part of $a \in \mathbb{C}$. Hence, we have

$$\int_0^\infty e^{-x^2 a} e^{-\mathrm{i}x\xi} \mathrm{d}x = \frac{1}{2}\left(\frac{\pi}{a}\right)^{\frac{1}{2}} e^{-\frac{\xi^2}{4a}} \left(1 + \operatorname{erf}\left(\frac{\mathrm{i}a^{-\frac{1}{2}}\xi}{2}\right)\right), \tag{3.6}$$

which implies

$$\begin{aligned}\int_{\mathbb{R}^{n-1}_+} e^{\mathrm{i}\boldsymbol{\xi}\cdot\mathbf{x}} e^{-|\mathbf{x}|^2(\mathrm{i}\sigma+\epsilon)} \mathrm{d}\mathbf{x} &= \int_0^\infty e^{\mathrm{i}\xi_1 x_1} e^{-x_1^2(\mathrm{i}\sigma+\epsilon)} \mathrm{d}x_1 \prod_{k=2}^{n-1} \left(\int_{\mathbb{R}} e^{\mathrm{i}\xi_k \cdot x_k} e^{-x_k^2(\mathrm{i}\sigma+\epsilon)} \mathrm{d}x_k \right) \\ &= \frac{1}{2}\left(\frac{\pi}{(\mathrm{i}\sigma+\epsilon)}\right)^{\frac{n-1}{2}} \left(1 + \operatorname{erf}\left(-\frac{1}{2}\mathrm{i}(\mathrm{i}\sigma+\epsilon)^{-\frac{1}{2}}\xi_1\right)\right) e^{-\frac{|\boldsymbol{\xi}|^2}{4(\mathrm{i}\sigma+\epsilon)}},\end{aligned}$$

with

$$\int_{\mathbb{R}} e^{-x^2 a} e^{-\mathrm{i}x\xi} \mathrm{d}x = \left(\frac{\pi}{a}\right)^{\frac{1}{2}} e^{-\frac{\xi^2}{4a}} \quad \text{for} \quad \operatorname{Re} a > 0. \tag{3.7}$$

Thus (3.4) is equal to

$$\int_0^\infty \mathcal{F}_{n-1}(R_H f)(\boldsymbol{\xi}, r) e^{r^2(-\mathrm{i}\sigma-\epsilon)} r^{n-1} \mathrm{d}r = \frac{1}{4}\left(\frac{\pi}{(\mathrm{i}\sigma+\epsilon)}\right)^{\frac{n-1}{2}} \left(1 + \operatorname{erf}\left(-\frac{\mathrm{i}\xi_1}{2(\mathrm{i}\sigma+\epsilon)^{\frac{1}{2}}}\right)\right) e^{-\frac{|\boldsymbol{\xi}|^2}{4(\mathrm{i}\sigma+\epsilon)}} \mathcal{F}_n F(\boldsymbol{\xi}, \sigma - \mathrm{i}\epsilon).$$

The compact support of F on the right-hand side implies the boundedness of $\mathcal{F}_n F$, which belongs to a Schwarz space, so the right-hand side has a finite value for every ϵ, which means it is bounded. Taking the limit on ϵ gives

$$\int_0^\infty \mathcal{F}_{n-1}(R_H f)(\boldsymbol{\xi}, r) e^{-\mathrm{i}r^2\sigma} r \mathrm{d}r = \frac{1}{4}\left(\frac{\pi}{\mathrm{i}\sigma}\right)^{\frac{n-1}{2}} \left(1 + \operatorname{erf}\left(-\frac{\mathrm{i}\xi_1}{2(\mathrm{i}\sigma)^{\frac{1}{2}}}\right)\right) e^{-\frac{|\boldsymbol{\xi}|^2}{4\mathrm{i}\sigma}} \mathcal{F}_n F(\boldsymbol{\xi}, \sigma),$$

or equivalently,

$$4\left(\frac{\mathrm{i}\sigma}{\pi}\right)^{\frac{n-1}{2}} \left(1 + \operatorname{erf}\left(-\frac{\mathrm{i}\xi_1}{2(\mathrm{i}\sigma)^{\frac{1}{2}}}\right)\right)^{-1} e^{-\frac{\mathrm{i}|\boldsymbol{\xi}|^2}{4\sigma}} \int_0^\infty \mathcal{F}_{n-1}(R_H f)(\boldsymbol{\xi}, r) e^{-\mathrm{i}r^2\sigma} r^{n-1} \mathrm{d}r = \mathcal{F}_n F(\boldsymbol{\xi}, \sigma).$$

Now, we can recover F by taking the inverse Fourier transform as

$$F(\mathbf{x}, z) = \frac{4}{(2\pi)^n} \int_{\mathbb{R}} \int_{\mathbb{R}^{n-1}} e^{\mathrm{i}\left(\mathbf{x}\cdot\boldsymbol{\xi} + z\sigma - \frac{|\boldsymbol{\xi}|^2}{4\sigma}\right)} \left(\frac{\mathrm{i}\sigma}{\pi}\right)^{\frac{n-1}{2}} \left(1 + \operatorname{erf}\left(-\frac{\mathrm{i}\xi_1}{2(\mathrm{i}\sigma)^{\frac{1}{2}}}\right)\right)^{-1} \times \int_0^\infty \mathcal{F}_{n-1}(R_H f)(\boldsymbol{\xi}, r) e^{-\mathrm{i}r^2\sigma} r^{n-1} \mathrm{d}r \mathrm{d}\boldsymbol{\xi} \mathrm{d}\sigma,$$

which implies the conclusion. □

To obtain the inversion of $R_L f$, we find the relation with the 2-dimensional quarter-spherical Radon transform $R_H f$ and then apply (3.1) with $n = 2$.

Theorem 4. *For $f \in C(\mathbb{R}^3)$ with compact support and $f(-\mathbf{x}, z) = -f(\mathbf{x}, z)$, we have*

$$f(\mathbf{x}, z) = \frac{\sqrt{\mathrm{i}}}{2\pi^{\frac{5}{2}}} \int_{\mathbb{R}} \int_{\mathbb{R}} e^{\mathrm{i}\left(z\xi + |\mathbf{x}|^2\sigma - \frac{\xi^2}{4\sigma}\right)} \left(1 + \operatorname{erf}\left(-\frac{\xi_1\sqrt{\mathrm{i}}}{2\sqrt{\sigma}}\right)\right)^{-1} \int_0^\infty \mathcal{F}_1(\partial_\theta R_L f)(\xi, \theta_{\mathbf{x}} - \pi/2, r) e^{-\mathrm{i}r^2\sigma} r^2 \sqrt{\sigma} \mathrm{d}r \mathrm{d}\xi \mathrm{d}\sigma,$$

where $\theta_{\mathbf{x}}$ is the polar angle of $\mathbf{x}$.

The assumption $f(-\mathbf{x}, z) = -f(\mathbf{x}, z)$ in the above Theorem 4 is necessary to prove it mathematically.

Proof. Notice that

$$R_L f(u, \theta, r) = \int_0^{\frac{\pi}{2}} \int_{\theta - \frac{\pi}{2}}^{\theta + \frac{\pi}{2}} f(r\cos\omega_1 \sin\omega_2, r\sin\omega_1 \sin\omega_2, r\cos\omega_2 + u) \sin\omega_2 \mathrm{d}\omega_1 \mathrm{d}\omega_2.$$

Differentiating with respect to θ gives

$$\partial_\theta R_L f(u, \theta, r) = \int_0^{\frac{\pi}{2}} \begin{bmatrix} f(r\cos(\theta + \frac{\pi}{2})\sin\omega_2, r\sin(\theta + \frac{\pi}{2})\sin\omega_2, r\cos\omega_2 + u) \\ -f(r\cos(\theta - \frac{\pi}{2})\sin\omega_2, r\sin(\theta - \frac{\pi}{2})\sin\omega_2, r\cos\omega_2 + u) \end{bmatrix} \sin\omega_2 \mathrm{d}\omega_2.$$

Let $F_\theta(\hat{x},\hat{z}) = [f(\hat{z}\cos(\theta+\frac{\pi}{2}),\hat{z}\sin(\theta+\frac{\pi}{2}),\hat{x}) - f(\hat{z}\cos(\theta-\frac{\pi}{2}),\hat{z}\sin(\theta-\frac{\pi}{2}),\hat{x})]\hat{z}, \hat{z}\geq 0$. Then, it follows that

$$r\partial_\theta R_L f(u,\theta,r) = R_H F_\theta(u,r),$$

where $R_H F_\theta$ is the 2-dimensional quarter-spherical Radon transform on the line. By exploiting (3.1) with $n=2$, we have, for $\hat{z}>0$,

$$\begin{aligned} &f\left(\hat{z}\cos(\theta+\frac{\pi}{2}),\hat{z}\sin(\theta+\frac{\pi}{2}),\hat{x}\right) - f\left(\hat{z}\cos(\theta-\frac{\pi}{2}),\hat{z}\sin(\theta-\frac{\pi}{2}),\hat{x}\right)\\ &= \frac{4}{(2\pi)^2}\int_{\mathbb{R}}\int_{\mathbb{R}} e^{\mathrm{i}\left(\hat{x}\xi+\hat{z}^2\sigma-\frac{|\xi|^2}{4\sigma}\right)}\left(\frac{\mathrm{i}\sigma}{\pi}\right)^{\frac{1}{2}}\left(1+\operatorname{erf}\left(-\frac{\xi_1\sqrt{\mathrm{i}}}{2\sqrt{\sigma}}\right)\right)^{-1}\int_0^\infty \mathcal{F}_1(\partial_\theta R_L f)(\xi,\theta,r)e^{-\mathrm{i}r^2\sigma}r^2\mathrm{d}r\mathrm{d}\xi\mathrm{d}\sigma, \end{aligned}$$

which implies the conclusion. □

4. Conclusion and additional remarks

In this paper, we studied two quarter-spherical Radon transforms which may arise in endoscopic PAT with a certain type of detectors. These spherical Radon transforms, one of the incomplete spherical Radon transforms, are first suggested and their exact inversion fomulas are provided. Considering applications of the spherical Radon transform, our results are expected to have a significant impact both mathematically and in terms of applicability in endoscopic PAT as well as sesimic waves, radar and PDEs.

Lastly, we would like to note the following:

1) Theorems 3 and 4 imply that the mapping $f \longmapsto R_H f$ is one-to-one on $C_c(\mathbb{R}^n) = \{f \in C(\mathbb{R}^n) : f \text{ has compact support}\}$ and the mapping $f \longmapsto R_L f$ is one-to-one on $\{f \in C_c(\mathbb{R}^3) : f(-\mathbf{x},z) = -f(\mathbf{x},z)\}$.
2) The smoothness and decay conditions for f in both inversion formulae (Theorems 3 and 4) are not optimized. This formula can hold under weaker requirements, such as piecewise continuity of f, or f decaying rapidly on the z axis.
3) Accurately and efficiently numerically implementing the inversion formula derived in the paper is an interesting problem in its own right. The authors plan to address this problem in future work.

Use of AI tools declaration

The authors declare they have not used Artificial Intelligence (AI) tools in the creation of this article.

Acknowledgments

The work of G. Hwang was supported by the 2020 Yeungnam University research grant. The work of S. Moon was supported by the National Research Foundation of Korea (NRF) grant funded by the Korea government (NRF-2022R1C1C1003464). We are thankful to the referees for multiple suggestions that helped to improve this paper. S. M. also thanks J. Lee, S. Mah and S. Park for fruitful discussions.

Conflict of interest

The authors declare that they have no competing interests.

References

1. G. Ambartsoumian, R. Gouia-Zarrad, V. P. Krishnan, S. Roy, Image reconstruction from radially incomplete spherical Radon data, *Eur. J. Appl. Math.*, **29** (2018), 470–493. https://doi.org/10.1017/S0956792517000250
2. L. Andersson, On the determination of a function from spherical averages, *SIAM J. Math. Anal.*, **19** (1988), 214–232. https://doi.org/10.1137/0519016
3. A. M. Cormack, Representation of a function by its line integrals, with some radiological applications, *J. Appl. Phys.*, **34** (1963), 2722–2727. https://doi.org/10.1063/1.1729798
4. A. M. Cormack, E. T. Quinto, A Radon transform on spheres through the origin in $\mathbb{R}^n$ and applications to the Darboux equation, *T. Am. Math. Soc.*, **260** (1980), 575–581. https://doi.org/10.1090/S0002-9947-1980-0574800-3
5. R. Courant, D. Hilbert, *Methods of mathematical physics*, New York: Interscience Publishers, 1962.
6. A. Erdelyi, *Tables of integral transforms*, New York: McGraw-Hill, 1954.
7. J. A. Fawcett, Inversion of *n*-dimensional spherical averages, *SIAM J. Appl. Math.*, **45** (1985), 336–341. https://doi.org/10.1137/0145018
8. D. Finch, S. K. Patch, Rakesh, Determining a function from its mean values over a family of spheres, *SIAM J. Math. Anal.*, **35** (2004), 1213–1240. https://doi.org/10.1137/S0036141002417814
9. D. Finch, Rakesh, Recovering a function from its spherical mean values in two and three dimensions, In: *Photoacoustic imaging and spectroscopy*, Florida: CRC Press, 2009.
10. I. M. Gelfand, S. G. Gindikin, M. I. Graev, *Selected Topics in Integral Geometry*, Providence: American Mathematical Society, 2003.
11. R. Gouia-Zarrad, S. Roy, S. Moon, Numerical inversion and uniqueness of a spherical Radon transform restricted with a fixed angular span, *Appl. Math. Comput.*, **408** (2021), 126338. https://doi.org/10.1016/j.amc.2021.126338
12. M. Haltmeier, Universal inversion formulas for recovering a function from spherical means, *SIAM J. Math. Anal.*, **46** (2014), 214–232. https://doi.org/10.1137/12088127
13. M. Haltmeier, S. Moon, The spherical Radon transform with centers on cylindrical surfaces, *J. Math. Anal. Appl.*, **448** (2017), 567–579. https://doi.org/10.1016/j.jmaa.2016.11.022
14. H. He, L. Englert, V. Ntziachrisos, Optoacoustic endoscopy of the gastrointestinal tract, *ACS Photonics*, **10** (2023), 559–570. https://doi.org/10.1021/acsphotonics.2c01264
15. R. G. M. Kolkman, E. Hondebrink, W. Steenbergen, T. G. van Leeuwen, F. F. M. de Mul, Photoacoustic imaging of blood vessels with a double-ring sensor featuring a narrow angular aperture, *J. Biomed. Opt.*, **9** (2004), 1327–1335. https://doi.org/10.1117/1.1805556

16. M. Kim, K. W. Lee, K. Kim, O. Gulenko, C. Lee, B. Keum, et al., Intra-instrument channel workable, optical-resolution photoacoustic and ultrasonic mini-probe system for gastrointestinal endoscopy, *Photoacoustics*, **26** (2022), 100346. https://doi.org/10.1016/j.pacs.2022.100346

17. P. Kuchment, *The Radon transform and medical imaging*, Philadelphia: SIAM, 2014.

18. L. Kunyansky, Inversion of the spherical means transform in corner-like domains by reduction to the classical Radon transform, *Inverse Probl.*, **31** (2015), 095001.

19. L. A. Kunyansky, A series solution and a fast algorithm for the inversion of the spherical mean Radon transform, *Inverse Probl.*, **23** (2007), S11. https://doi.org/10.1088/0266-5611/23/6/S02

20. L. A. Kunyansky, Fast reconstruction algorithms for the thermoacoustic tomography in certain domains with cylindrical or spherical symmetries, *Inverse Probl. Imag.*, **6** (2012), 111–131.

21. M. M. Lavrent'ev, V. G. Romanov, S. P. Shishatskii, *Ill-posed problems of mathematical physics and analysis*, Providence: American Mathematical Society, 1986.

22. Y. Li, G. Lu, Q. Zhou, Z. Chen, Advances in endoscopic photoacoustic imaging, *Photonics*, **8** (2021), 281. https://doi.org/10.3390/photonics8070281

23. N. N. Lebedev, R. A. Silverman, *Special functions and their applications*, New York: Dover Publications, 2012.

24. S. Moon, Inversion formulas and stability estimates of the wave operator on the hyperplane, *J. Math. Anal. Appl.*, **466** (2018), 490–497. https://doi.org/10.1016/j.jmaa.2018.06.006

25. S. Moon, Inversion of the spherical Radon transform on spheres through the origin using the regular Radon transform, *Commun. Pur. Appl. Anal.*, **15** (2016), 1029–1039. https://doi.org/10.3934/cpaa.2016.15.1029

26. S. Moon, Orthogonal function series formulas for inversion of the spherical Radon transform, *Inverse Probl.*, **36** (2020), 035007. https://doi.org/10.1088/1361-6420/ab6d54

27. E. K. Narayanan, Rakesh, Spherical means with centers on a hyperplane in even dimensions, *Inverse Probl.*, **26** (2010), 035014. https://doi.org/10.1088/0266-5611/26/3/035014

28. F. Natterer, Photo-acoustic inversion in convex domains, *Inverse Probl. Imag.*, **2** (2012), 315–320. https://doi.org/10.3934/ipi.2012.6.315

29. C. J. Nolan, M. Cheney, Synthetic aperture inversion, *Inverse Probl.*, **18** (2002), 221. https://doi.org/10.1088/0266-5611/18/1/315

30. E. T. Quinto, Null spaces and ranges for the classical and spherical Radon transforms, *J. Math. Anal. Appl.*, **90** (1982), 408–420. https://doi.org/10.1016/0022-247X(82)90069-5

31. Rakesh, T. Yuan, Recovering initial values from light cone traces of solutions of the wave equation, *Inverse Probl.*, **34** (2018), 075003. https://doi.org/10.1088/1361-6420/aabf0e

32. N. J. Redding, G. N. Newsam, *Inverting the circular Radon transform*, DSTO Electronics and Surveillance Research Laboratory, Edinburgh, South Australia, 2001.

33. T. A. Syed, V. P. Krishnan, J. Sivaswamy, Numerical inversion of circular arc Radon transform, *IEEE T. Comput. Imag.*, **2** (2016), 540–549. https://doi.org/10.1109/TCI.2016.2615806

34. Z. Sun, H. Sun, Image reconstruction for endoscopic photoacoustic tomography including effects of detector responses, *Exp. Biol. Med.*, **247** (2022), 881–897. https://doi.org/10.1177/15353702221079570

35. M. Xu, G. Ku, L. V. Wang, Microwave-induced thermoacoustic tomography using multi-sector scanning, *Med. Phys.*, **28** (2001), 1958–1963. https://doi.org/10.1118/1.1395037

36. M. Xu, L. V. Wang, Universal back-projection algorithm for photoacoustic computed tomography, *Phys. Rev. E*, **71** (2005), 016706. https://doi.org/10.1103/PhysRevE.71.016706

37. J. M. Yang, K. Maslov, H. C. Yang, Q. Zhou, K. K. Shung, L. V. Wang, Photoacoustic endoscopy, *Opt. Lett.*, **34** (2009), 1591–1593. https://doi.org/10.1364/OL.34.001591

38. C. E. Yarman, B. Yazici, Inversion of the circular averages transform using the Funk transform, *Inverse Probl.*, **27** (2011), 065001. https://doi.org/10.1088/0266-5611/27/6/065001

39. L. Zalcman, Offbeat integral geometry, *Am. Math. Mon.*, **87** (1980), 161–175. https://doi.org/10.1080/00029890.1980.11994985

40. G. Zangerl, S. Moon, M. Haltmeier, Photoacoustic tomography with direction dependent data: an exact series reconstruction approach, *Inverse Probl.*, **35** (2019), 114005. https://doi.org/10.1088/1361-6420/ab2a30

41. S. Zheng, Q. Meng, X. Y. Wang, Quantitative endoscopic photoacoustic tomography using a convolutional neural network, *Appl. Opt.*, **61** (2022), 2574–2581. https://doi.org/10.1364/AO.441250

AIMS Press